
DISTRIBUTED SPARSE SGD WITH MAJORITY VOTING

Kerem Ozfatura¹ Emre Ozfatura² Deniz Gündüz²

ABSTRACT

Distributed learning, particularly variants of distributed stochastic gradient descent (DSGD), are widely employed to speed up training by leveraging computational resources of several workers. However, in practise, communication delay becomes a bottleneck due to the significant amount of information that needs to be exchanged between the workers and the parameter server. One of the most efficient strategies to mitigate the communication bottleneck is top- K sparsification. However, top- K sparsification requires additional communication load to represent the sparsity pattern, and the mismatch between the sparsity patterns of the workers prevents exploitation of efficient communication protocols. To address these issues, we introduce a novel majority voting based sparse communication strategy, in which the workers first seek a consensus on the structure of the sparse representation. This strategy provides a significant reduction in the communication load and allows using the same sparsity level in both communication directions. Through extensive simulations on the CIFAR-10 dataset, we show that it is possible to achieve up to $\times 4000$ compression without any loss in the test accuracy.

1 INTRODUCTION

Advances in the design of neural network (NN) architectures exhibit impressive results in many challenging classification problems (Simonyan & Zisserman, 2015; He et al., 2016; He et al., 2016; Huang et al., 2017). However, these designs mainly promote deeper NN structures, which come at the cost of significant training time, as they also require much larger datasets for training. As a result, training these deep NNs (DNNs) has become a formidable task that is increasingly infeasible to perform on a single machine within a reasonable time frame. The solution is to employ a distributed training framework, where multiple machines/workers are used in parallel to reduce the training time under the supervision of a parameter server (Dean et al., 2012; Dekel et al., 2012; Zinkevich et al., 2010; Li et al., 2014).

From a theoretical point of view parameter server type implementations, such as synchronous parallel stochastic gradient descent (SGD), offer a speed up of training that scales linearly with the number of workers. However, such a speed up is typically not possible in practise as distributed training requires exchange of large amounts of information between the parameter server and the workers, and the communication latency becomes the bottleneck. The communication bottleneck becomes particularly pertinent when the com-

munication is performed over bandwidth limited channels, for example, when the workers are edge devices (Abad et al., 2020; Wang et al., 2019). Numerous techniques have been proposed in the recent years to reduce the communication load in distributed learning. Next, we briefly explain the general distributed SGD (DSGD) framework, and then briefly overview some of the popular strategies to reduce the communication load.

1.1 Preliminaries

Many parameterized machine learning problems can be modeled as a *stochastic optimization problem*

$$\min_{\theta \in \mathbb{R}^d} := \mathbb{E}_{\zeta \sim \mathcal{D}} F(\theta, \zeta), \quad (1)$$

where $\theta \in \mathbb{R}^d$ denotes the model parameters, ζ is the random data sample, \mathcal{D} denotes the data distribution, and the F is the problem specific empirical loss function. Stochastic optimization problem given above can be solved in a distributed manner over N workers by rewriting the minimization problem in (1) as

$$\min_{\theta \in \mathbb{R}^d} f(\theta) = \frac{1}{N} \sum_{n=1}^N \underbrace{\mathbb{E}_{\zeta \sim \mathcal{D}_n} F_n(\theta, \zeta)}_{:= f_n(\theta)}, \quad (2)$$

where \mathcal{D}_n denotes the portion of the dataset allocated to worker n . Most machine learning algorithms employ SGD for the solution of the above problem. In PS-type implementation of DSGD, at the beginning of iteration t , each worker pulls the current global parameter model θ_t from the PS and

¹Department of Computer Science, Ozyegin University, Istanbul, Turkey ²Information Processing and Communications Lab, Dept. of Electrical and Electronic Engineering, Imperial College London, London, UK. Correspondence to: Kerem Ozfatura <kerem.ozfatura@ozu.edu.tr>.

computes the *local stochastic gradient*

$$\mathbf{g}_{n,t} = \nabla_{\boldsymbol{\theta}_t} F_n(\boldsymbol{\theta}_t, \zeta_{n,t}), \quad (3)$$

where $\zeta_{n,t}$ is the sampled training data at iteration t by the n th worker. Then, each worker sends (pushes) the value of its local gradient estimate to the PS, where those values are aggregated to update the parameter model, i.e.,

$$\boldsymbol{\theta}_{t+1} = \boldsymbol{\theta}_t - \eta_t \underbrace{\frac{1}{N} \sum_{n=1}^N \mathbf{g}_{n,t}}_{\mathbf{G}_t}, \quad (4)$$

where η_t is the learning rate.

1.2 Communication efficient distributed learning

There is a plethora of works on communication efficient distributed learning, which can be classified into three main categories; namely, sparsification, quantization, and local SGD. Let \mathbf{g} denote the generic gradient estimate to be transmitted from a worker to the parameter server at some iteration of the DGSD algorithm.

1.2.1 Quantization

The objective of the quantization strategy is to represent \mathbf{g} with as few bits as possible. Without quantization, each element is represented with 32 bits according to the floating point precision. The typical approach is to employ scalar quantization, where each value of \mathbf{g} is quantized into fewer than 32 bits. In the other extreme, each element of \mathbf{g} can be represented by a single bit (Bernstein et al., 2018; 2019). Numerous quantization strategies have been studied in the literature for the DSGD framework (Zheng et al., 2019; Alistarh et al., 2017; Wen et al., 2017; Wu et al., 2018b; Seide et al., 2014).

1.2.2 Sparsification

The core idea behind sparse communication is to obtain a sparse version of the vector \mathbf{g} , denoted by $\tilde{\mathbf{g}}$, such that at most ϕ portion of the values in $\tilde{\mathbf{g}}$ are non zero, i.e.,

$$\|\tilde{\mathbf{g}}\|_1 \leq \phi \cdot d, \quad (5)$$

where d is the dimension of \mathbf{g} . Then, only the non-zero values in $\tilde{\mathbf{g}}$ are transmitted to the parameter server. In general, $\tilde{\mathbf{g}}$ is represented using a sparsity mask $\mathbf{M} \in \{0, 1\}^d$, such that $\tilde{\mathbf{g}} = \mathbf{M} \otimes \mathbf{g}$, where \otimes denotes element-wise multiplication. The key challenges for sparse communication is the design of the sparsity mask \mathbf{M} , and the representation of the positions of its non-zero entries with minimum number of bits. Recent works have shown that employing sparse communication with $\phi \in [0.01, 0.001]$ while training DNN architectures, such as ResNet or VGG,

reduces the communication load significantly without a notable degradation in the accuracy performance (Lin et al., 2018; Stich et al., 2018; Alistarh et al., 2018; Wangni et al., 2018; Aji & Heafield, 2017; Shi et al., 2019; Jiang & Agrawal, 2018; Barnes et al., 2020; Sattler et al., 2019).

1.2.3 Local SGD

Another common strategy to reduce the communication load is local SGD. While the previous two strategies aim to reduce the number of bits sent at each communication round, local SGD aims to minimize the total number of communication rounds by simply allowing each worker to update its model locally for H consecutive SGD steps (Stich, 2019; Lin et al., 2020b; Zhou & Cong, 2018; Yu et al., 2019a; Wang & Joshi, 2018; Yu et al., 2018; Haddadpour et al., 2019; Dieuleveut & Patel, 2019; Khaled et al., 2020). This implies $\times H$ reduction in the number of communication rounds compared to standard DSGD. Local SGD mechanism is also one of the key features of the popular federated learning framework (McMahan et al., 2017).

1.3 Motivation and Contributions

For communication efficient distributed learning, one of the most efficient and widely used strategies is the top- K sparsification framework, especially when it is implemented together with the error feedback/accumulation mechanism. However, there are certain drawbacks of the top- K sparsification framework. First, although sparsification reduces the number of parameter values to be transmitted at each communication round, it requires the transmission of additional bits to identify the positions of non-zero entries in sparse representations. Second, since the positions of the top- K values do not necessarily match across the workers, top- K sparsification is not a linear operation. However, since the ultimate aim at the parameter server is to compute the average of the gradient estimates over all the workers, instead of receiving each one separately, linearity property can help to employ more efficient communication strategies both in wired (Eghlidi & Jaggi, 2020) and wireless network setups (Mohammadi Amiri & Gündüz, 2020; Sery & Cohen, 2020; Zhu et al., 2019). Finally, another disadvantage of the mismatch between the top- K positions among the workers is that the promised sparsification level is only satisfied at the uplink direction.

To overcome these limitations, we introduce a majority voting based sparse communication strategy building upon the top- K sparsification framework with an additional consensus mechanism, where all the workers agree on the structure of the sparsity. Furthermore, we show that by establishing a certain correlation between the non-sparse positions of the gradient estimates observed in consecutive iterations, the

proposed voting scheme can be modified to utilize this correlation and achieve a lower communication load, measured in terms of the total number of transmitted bits, which is critical when the quantization and sparsification strategies are employed together.

Beyond communication efficiency, we also want to establish a relationship between the sparsity of the NN architecture obtained as a result of the distributed training process, and the sparsity used for communication. In other words, we explore if a tailored sparsification strategy for communication can exploit the sparse nature of the NN architecture, similarly to network pruning (Mostafa & Wang, 2019; Franke & Carbin, 2019; Lin et al., 2020a). Indeed, as further highlighted in Section 4, we observe that sparse communication can also result in improved accuracy results; hence, we argue that a sparse communication strategy that is aligned with the sparse nature of the NN architecture may help to achieve better generalization.

2 SPARSE COMMUNICATION WITH MAJORITY VOTING

One of the most commonly used techniques for communication efficient DSGD is top- K sparsification. Let $\mathbf{g}_{n,t}$ denote the local gradient estimate computed by the n th worker at iteration t . The worker sends a sparse version of its gradient estimate $\mathbf{g}_{n,t}$, denoted by $\tilde{\mathbf{g}}_{n,t}$, by keeping only the K largest absolute values. That is,

$$\tilde{\mathbf{g}}_{n,t} = \mathbf{g}_{n,t} \otimes \mathbf{M}_{n,t}, \quad (6)$$

where $\mathbf{M}_{n,t} = S_{top}(\mathbf{g}_{n,t}, K)$ is the sparsity mask used by the n th worker. Here, $S_{top}(\mathbf{g}, K)$ returns a vector with K ones corresponding to the K elements of vector \mathbf{g} with the highest absolute values. Accordingly, the PS aggregates the sparse gradients $\tilde{\mathbf{g}}_{1,t}, \dots, \tilde{\mathbf{g}}_{N,t}$ from the N workers to obtain the global gradient estimate $\tilde{\mathbf{G}}_t \triangleq \frac{1}{N} \sum_{n=1}^N \tilde{\mathbf{g}}_{n,t}$, which is then used to update the global model, i.e.,

$$\boldsymbol{\theta}_{t+1} = \boldsymbol{\theta}_t + \eta_t \tilde{\mathbf{G}}_t. \quad (7)$$

The key design objective of top- K sparsification is to reduce the communication load in the uplink direction, i.e., from the workers to the parameter server; thus the sparsification levels in the uplink and downlink directions do not necessarily match, and different sparsification masks can be employed.

We remark that if all the workers use the same sparsity mask, i.e., $\mathbf{M}_{n,t} = \mathbf{M}_t, \forall n$, then the sparsification becomes a linear operation; that is,

$$\tilde{\mathbf{G}}_t = \mathbf{G}_t \otimes \mathbf{M}_t = \frac{1}{N} \sum_{n=1}^N \mathbf{g}_{n,t} \otimes \mathbf{M}_t = \frac{1}{N} \sum_{n=1}^N (\mathbf{g}_{n,t} \otimes \mathbf{M}_t). \quad (8)$$

This linearity property can be utilized to employ more efficient collective operations in the distributed setup, such as using *all-reduce* operation instead of *all-gather* (Eghlidi & Jaggi, 2020), or to take advantage of the superposition property of wireless channels (Sery & Cohen, 2020; Mohammadi Amiri & Gündüz, 2020; Zhu et al., 2019) when the workers are edge devices.

In addition to aforementioned discussion on efficient sparse communication, we also argue that using a common sparsity mask, besides reducing the communication load, can also allow exploiting the sparse nature of the deep NN architectures; and hence, achieve better generalization and higher test accuracy. Later, by conducting extensive simulations, we show that inducing sparsity with a certain structure for communication can indeed help to achieve better generalization performance.

In this work, we want to design a computationally efficient mechanism to construct a global sparsity mask \mathbf{M}_t at each iteration t . Inspired by (Bernstein et al., 2019), we introduce a *majority voting (MV)* based mechanism to construct the global sparsity matrix, which, in a broad sense, corresponds to jointly identifying the most important K locations for the global model update across all the workers.

The voting mechanism is executed in the following way: at each iteration t , each worker computes the local gradient estimate $\mathbf{g}_{n,t}$, and identifies the largest K absolute values $\mathbf{M}_{n,t} = S_{top}(|\mathbf{g}_{n,t}|, K)$, and sends the locations of the non-zero entries of $\mathbf{M}_{n,t}$, denoted by $\text{supp}(\mathbf{M}_{n,t})$, to the PS as its vote. The PS collects all the votes, and counts the votes for all the positions to observe the most voted K positions, which form the global sparsity mask. Hence, the sparsity mask can be written as

$$\mathbf{M}_t = S_{top} \left(\sum_{n=1}^N S_{top}(|\mathbf{g}_{n,t}|, K), K \right). \quad (9)$$

Once the mask \mathbf{M}_t is constructed, it is communicated to all the workers. Each worker sends a sparsified version of its local gradient estimate using the global mask, i.e., worker n sends $\mathbf{g}_{n,t} \otimes \mathbf{M}_t$ to the PS to be aggregated. We call this scheme *sparse SGD with majority voting (SSGD-MV)*.

We want to highlight that, although we consider a two-step process, the total number of transmitted bits in the uplink direction is the same with top- K sparsification, and less number of bits are transmitted in the downlink direction. Later in Section 3, we will introduce a more efficient voting mechanism by utilizing the correlation among the gradient estimates over time, so that the number of transmitted bits in the uplink direction during the voting stage can be reduced.

Before giving the detailed analysis of the SSGD-MV scheme, we note that the proposed strategy can also be employed in the local SGD framework, in which each worker

performs multiple local updates before communicating with the PS. Hence, we consider the general setup, where each worker performs H local iterations, then sends the corresponding local model difference to the PS for aggregation and model update. The model difference of the n th worker at iteration t can be written as

$$\Delta\theta_{n,t} = \sum_{h=1}^H -\eta_t \mathbf{g}_{n,t}^{(h)}, \quad (10)$$

where

$$\mathbf{g}_{n,t}^{(h)} = \nabla_{\theta} F_n(\theta_{n,t}^{(h)}, \zeta_{n,t}), \quad (11)$$

and

$$\theta_{n,t}^{(h)} = \theta_{n,t}^{(i-1)} - \eta_t \mathbf{g}_{n,t}^{(h)}. \quad (12)$$

Here, we have set $\theta_{n,t}^{(0)} = \theta_t$.

The overall procedure of SSGD-MV is illustrated in Algorithm 1. It has been shown that error accumulation/feedback technique combined with sparsification achieves better convergence results (Stich et al., 2018; Karimireddy et al., 2019; Wu et al., 2018a; Tang et al., 2019; Yu et al., 2019b). Hence, we employ the error accumulation strategy such that worker n keeps track of the sparsification error, $\mathbf{e}_{n,t-1}$ at iteration t , to be aggregated to the local model difference $\Delta_{n,t}$ of the next iteration as illustrated in line 9 and line 22 of Algorithm 1.

In Algorithm 1, we consider two possible strategies to decide the winning locations of the voting procedure; the first one (highlighted with blue) simply counts the received votes from the workers and selects the top- K most voted entries. Instead, in the second strategy, called majority voting with random selection (SSGD-MV-RS) (highlighted with red), the winning locations are sampled randomly according to a distribution whose probabilities are proportional to the received votes. We note that the motivation behind the random selection strategy is to reduce any bias, similarly to the designs in (Barnes et al., 2020; Elibol et al., 2020).

Next, we analyze the communication load of the proposed SSGD-MV strategy.

2.1 Communication Load Analysis

To measure the communication load, we use the total number of transmitted bits per iteration per users, denoted by Q . We note that Q can be written as the sum of two quantities, Q^{up} and Q^{down} , which correspond to uplink and downlink communication loads, respectively. Further, both Q^{up} and Q^{down} are equal to the sum of two terms, where the first one, $Q_{loc}^{up}/Q_{loc}^{down}$, corresponds to the number of bits used for majority voting to identify the non-zero positions, while the second one, $Q_{val}^{up}/Q_{val}^{down}$, is the number of bits used to transmit corresponding values.

Algorithm 1 Sparse SGD with Majority Voting

```

1: for  $t = 1, \dots, T$  do
2:   Voting phase worker side:
3:   for  $n = 1, \dots, N$  do
4:     Receive  $\tilde{\Delta}_{t-1}$  from PS
5:     Update model:  $\theta_t = \theta_{t-1} + \tilde{\Delta}_{t-1}$ 
6:     initialize  $\theta_{n,t}^{(0)} = \theta_t$ 
7:     Perform  $H$  local SGD steps:
8:      $\Delta_{n,t} = \theta_{n,t}^{(H)} - \theta_{n,t}^{(0)}$ 
9:      $\bar{\Delta}_{n,t} = \Delta_{n,t} + \mathbf{e}_{n,t}$ 
10:     $\mathbf{M}_{n,t} = S_{top}(|\bar{\Delta}_{n,t}|, K)$ 
11:    Send  $\text{supp}(\mathbf{M}_{n,t})$  to PS
12:  end for
13:  Voting phase PS side:
14:  Apply majority voting:
15:   $\mathbf{M}_t = S_{top}(\sum_{n=1}^N \mathbf{M}_{n,t}, K)$ 
16:   $\mathbf{M}_t = S_{rand-weighted}(\sum_{n=1}^N \mathbf{M}_{n,t}, K)$ 
17:  Send  $\text{supp}(\mathbf{M}_t)$  to workers
18:  Sparse communication worker side:
19:  for  $n = 1, \dots, N$  do
20:     $\tilde{\Delta}_{n,t} = \mathbf{M}_t \otimes \Delta_{n,t}$ 
21:    Send  $\tilde{\Delta}_{n,t}$  to PS
22:     $\mathbf{e}_{n,t+1} = \bar{\Delta}_{n,t} - \tilde{\Delta}_{n,t}$ 
23:  end for
24:  Sparse communication PS side:
25:  Aggregate local sparse gradients:
26:   $\tilde{\Delta}_t = \sum_{n \in [N]} \tilde{\Delta}_{n,t}$ 
27:  send  $\tilde{\Delta}_t$  to all workers
28: end for

```

Given the sparsity parameter $K = \phi \cdot d$, one can observe that

$$Q_{val}^{up} = Q_{val}^{down} = q\phi d, \quad (13)$$

where q is the number of bits to represent each value according to the chosen quantization framework. Its default value is $q = 32$, corresponding to 32 bits floating point precision.

For the voting phase, each non-zero position can be represented with $\log(d)$ bits, in the most naive approach, which implies $Q_{loc}^{up} = Q_{loc}^{down} = d\phi \log d$. However, as we later illustrate in Section 4.3, the total number of bits required to represent the positions of non-zero locations can be reduced to

$$Q_{loc}^{up} = Q_{loc}^{down} = d\phi(\log(1/\phi) + 2). \quad (14)$$

Consequently, the number of bits transmitted in both the uplink and downlink directions is given by

$$Q^{up} = Q^{down} = \phi d(\log(1/\phi) + q + 2). \quad (15)$$

One can easily observe from (15) that, depending on the choice of the sparsification ratio ϕ and the number of bits

to represent each model difference value q , transmission of the non-zero positions or the non-zero values may become the bottleneck. In other words, if the precision of the quantization, thus the number of required bits q , is reduced, then the voting mechanism will become the bottleneck in the communication load, thus the impact of the quantization technique will be limited by the voting phase. For instance, when $\phi = 10^{-2}$, 9 bits are required to represent the position of each non-zero value; therefore, when $q < 9$, the communication load will be dominated by the voting phase.

Hence, in order to utilize the quantization technique effectively, there is a need for a more efficient voting mechanism, particularly in the uplink direction. To this end, we introduce a more efficient voting mechanism in the next subsection, which builds upon the assumption that the most important NN parameters, those demonstrating more visible changes in their values, do not change radically through the training process, which, in our setup, implies that the votes of the workers will be correlated temporally.

3 MAJORITY VOTING WITH TIME CORRELATION

In this section, we introduce a new voting mechanism to construct the sparsity mask, called majority voting with add-drop (SSGD-MV-AD), which builds upon the aforementioned heuristic that locations of the NN parameters that exhibit larger variations are correlated over iterations. Hence, our objective is to modify the voting process in order to utilize this correlation and reduce the required number of bits that must be communicated in the voting phase.

To this end, we propose an *add-drop* mechanism for the voting phase. In the original majority voting mechanism, each worker sends the locations of the largest K absolute values, where K corresponds to the ϕ portion of the total gradient dimension. When the add-drop mechanism is employed, the current vote of each worker is obtained by changing only a certain portion of the its previous vote. Hence, at each iteration, each worker sends the list of indices to be removed/added to the previously voted indices. We use K_{ad} to denote the maximum number of changes allowed during voting; that is, at each iteration at most K_{ad} number of indices can be removed/added to the voting list by each worker, which corresponds to $\phi_{ad} \ll \phi$ portion of all the parameters.

Let $\tilde{\mathbf{M}}_{n,t}$ denote the votes of worker n at iteration t according to the add-drop mechanism, which can be executed in the following way: to obtain the indices to be added at iteration t , worker n identifies the largest K_{ad} absolute values in the current top- K values $\mathbf{M}_{n,t}$ that are not present in the previous vote $\tilde{\mathbf{M}}_{n,t-1}$ (as illustrated in line 14 of Algorithm 2), and similarly, to obtain the indices to be removed at iteration

Algorithm 2 Majority Voting with Add-Drop (MV-AD)

```

1: for  $t = 1, \dots, T$  do
2:   Voting phase worker side:
3:   for  $n = 1, \dots, N$  do
4:     Receive  $\tilde{\Delta}_{t-1}$  from PS
5:     Update model:  $\theta_t = \theta_{t-1} + \tilde{\Delta}_{t-1}$ 
6:     initialize  $\theta_{n,t}^{(0)} = \theta_t$ 
7:     Perform local SGD for  $H$  iterations:
8:      $\Delta_{n,t} = \theta_{n,t}^{(H)} - \theta_{n,t}^{(0)}$ 
9:      $\tilde{\Delta}_{n,t} = \Delta_{n,t} + \mathbf{e}_{n,t}$ 
10:     $\mathbf{M}_{n,t} = S_{top}(|\tilde{\Delta}_{n,t}|, K)$ 
11:    Add-drop mechanism:
12:     $\mathbf{M}_{n,t}^{add} =$ 
13:       $S_{top}(\max((\mathbf{M}_{n,t} - \tilde{\mathbf{M}}_{n,t-1}), 0) \otimes \tilde{\Delta}_{n,t}, K_{ad})$ 
14:     $\mathbf{M}_{n,t}^{drop} =$ 
15:       $S_{bot}(\max((\tilde{\mathbf{M}}_{n,t-1} - \mathbf{M}_{n,t}), 0) \otimes \tilde{\Delta}_{n,t}, K_{ad})$ 
16:     $\tilde{\mathbf{M}}_{n,t} = \tilde{\mathbf{M}}_{n,t-1} + \mathbf{M}_{n,t}^{add} - \mathbf{M}_{n,t}^{drop}$ 
17:  end for
18:  Voting phase PS side:
19:  Apply voting
20:   $\mathbf{M}_t^{sum} = \mathbf{M}_{t-1}^{sum} + \sum_{n=1}^N (\mathbf{M}_{n,t}^{add} - \mathbf{M}_{n,t}^{drop})$ 
21:  Count the votes:
22:   $\mathbf{M}_t = S_{top}(\mathbf{M}_t^{sum}, K)$ 
23:  Send  $\mathbf{M}_t$  to workers
24:  Sparse communication worker side:
25:  for  $n = 1, \dots, N$  do
26:     $\tilde{\Delta}_{n,t} = \mathbf{M}_t \otimes \tilde{\Delta}_{n,t}$ 
27:    Send  $\tilde{\Delta}_{n,t}$  to PS
28:     $\mathbf{e}_{n,t} = \tilde{\Delta}_{n,t} - \tilde{\Delta}_{n,t}$ 
29:  end for
30:  Sparse communication PS side:
31:  Aggregate local sparse model updates:
32:   $\tilde{\Delta}_t = \sum_{n \in [N]} \tilde{\Delta}_{n,t}$ 
33:  send  $\tilde{\Delta}_t$  to all workers
34: end for

```

tion t , worker n identifies the K_{ad} lowest absolute values in the previous vote $\tilde{\mathbf{M}}_{n,t-1}$ that are not in the current top- K values $\mathbf{M}_{n,t}$ (as illustrated in line 12 of the algorithm 2).

We remark that the PS does not need to keep track of the previous votes of the all workers. As illustrated in Algorithm 2 (line 20), it is sufficient to keep track of the cumulative sum of the votes \mathbf{M}_t^{sum} , which is updated according to the following rule:

$$\mathbf{M}_t^{sum} = \mathbf{M}_{t-1}^{sum} + \sum_{n=1}^N (\mathbf{M}_{n,t}^{add} - \mathbf{M}_{n,t}^{drop}). \quad (16)$$

If we revisit our example scenario where $\phi = 10^{-2}$ and set $\phi_{ad} = 10^{-3}$, which corresponds to assuming 90% correlation over time, the number of bits required to represent each

position will now be 12 bits, but the number of transmitted positions will be reduced by a factor of 5; hence, effectively the number of bits per position will be only 2.4.

We want to highlight that, although the main design goal of the add-drop mechanism is to reduce the communication load of the voting mechanism, in parallel it also functions similarly to the network pruning strategy. In a sense, it naturally seeks a sparse version of the NN architecture since the add-drop mechanism enforces training along a direction dictated by a small subset of the parameters.

4 NUMERICAL RESULTS

4.1 Simulation Setup

To evaluate the performance of the proposed majority voting strategies, we consider the image classification task on the CIFAR-10 dataset (Krizhevsky et al.), which consists of 10 RGB image classes, and 50K training and 10K test images, respectively. For the training, we choose ResNet-18 neural network architecture (He et al., 2016), which consists of 8 basic blocks, each with two 3x3 convolutional layers and batch normalization. After two consecutive basic blocks, image size is halved with an additional 3x3 convolutional layer employing stride. This network consists of 11,173,962 trainable parameters altogether. We consider $N = 10$ workers, and a federated setup, where the available training dataset is divided among the workers in a disjoint manner. The images, based on their classes, are distributed in an identically and independently distributed (IID) manner among the workers.

4.2 Simulation Scenario

We have implemented the proposed three novel algorithms, and tested them with different numbers of local gradient iterations and quantization methods. These algorithms are i) SSGD-MV, ii) SSGD-MV-AD, and iii) SSGD-MV-RS. To compare with these algorithms we also implemented sparse SGD with top- K batch and single machine (SM) benchmark. Each variation of the simulation results is an average of 10 separate trails, apart from SSGD-MV-RS, whose results are averaged across 5 separate trials for each of its own variations.

In the presentation of our numerical results, we denote the number of local steps H with LH , and if we apply quantization to the algorithm, we denote it only by adding a Q symbol, as we only utilize 4 bit quantization. For example, SSGD-MV-L4-Q stands for quantized sparse SGD with majority voting with $H = 4$ local iterations.

In SSGD-MV, we took the indices of the top $\phi = 10^{-2}$

absolute model difference values from the PS model, after the H -th local model update, where we experimented with $H = 2, 4, 8$. Each worker creates a mask based on its top $\phi = 10^{-2}$ parameters, and sends its support to the parameter server which is where we apply majority voting system to make a global mask which is used by all workers to send the masked selected parameters.

Unlike SSGD-MV, where each worker votes for the ratio of $\phi = 10^{-2}$ parameters, in SSGD-MV-AD, workers only make 10% change in their previous vote; specifically $\phi_{add} = 10^{-3}$ to add new voted parameters and $\phi_{drop} = 10^{-3}$ remove from the previous vote. Workers make those changes at the end of H -th local iteration. When all workers communicate their masks, parameter server computes the new global mask by utilizing majority voting system.

In SSGD-MV-RS, the parameter server calculates the global mask by randomly selecting the indices using the votes until $\phi = 10^{10-2}$ number of unique indices are selected. Due to the algorithm’s nature, if a certain index is voted by an overwhelming majority, it has a higher chance of being selected for the global mask.

We set starting learning rate to $\eta = 0.5$ for all the experiments aside of the SM benchmark which we set starting learning rate to $\eta = 0.1$.

In all the implementations we employ the warm up strategy (Goyal et al., 2017), where the learning rate is initially set to $\eta = 0.1$, and is increased to its corresponding scaled value gradually in the first 5 epochs. We also note that, we do not employ the sparsification and quantization methods during the warm up phase.

In all the simulations, the DNN architecture is trained for 300 epochs and the learning rate is reduced by a factor of 10 after the first 150 and 225 epochs, respectively (He et al., 2016; He et al., 2016). Lastly, in all the simulations we employ L2 regularization with a given weight decay parameter 10^{-4} .

4.3 Sparse and Quantized Representation

Here, we will briefly explain how we represent the non-zero positions of a sparse vector and its quantized values.

4.3.1 Sparse representation

The position of each non-zero value can be represented using $\log(d)$ bits. However, as the size of the DNN architectures are taken into account, with millions of parameters, this

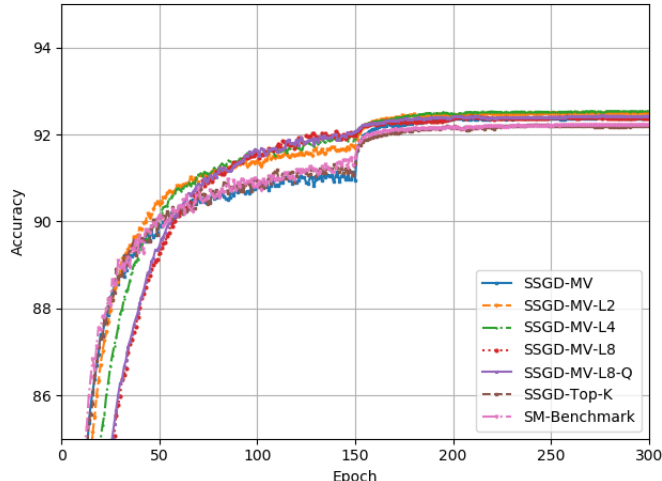


Figure 1. Test accuracy results over 300 epochs for SSGD-MV variations, SSGD-top- K and SM benchmark

means more than 20 bits for each non-zero position. Instead, we propose an alternative method to represent the non-zero positions. In which the number of bits per each non-zero location is not a parameter of d , but the sparsification ratio ϕ .

For a given sparse vector \mathbf{g} with a sparsity ratio of ϕ , the proposed sparse representation strategy works in the following way. First, \mathbf{g} is divided into blocks of size $1/\phi$, which creates $d\phi$ equal-length blocks. Within each block, the positions of non-zero values can be represented using $\log(1/\phi)$ bits. Now, to complete the sparse representation of the vector, we need an identifier for the end of each block, hence we use a one-bit symbol, i.e., 0, to indicate the end of block. Accordingly, we append a one-bit symbol, i.e., 1, to the beginning of each $\log(1/\phi)$ bits used for the intra-block positioning.

Once the sparse representation is sent, receiver starts reading from the beginning of the bit stream and if the initial bit is 1, then reads the next $\log(1/\phi)$ bits to recover the intra-block position and move the cursor accordingly, if the initial bit is 0, then updates the block index and moves the cursor accordingly, this process is continued until the cursor reaches the end of the bit stream. From the communication aspect, on the average, $\log(1/\phi) + 2$ bits are used for position of the each non-zero value. To clarify with an example, when $\phi \in [1/64, 1/128]$, 9 bits are sufficient for the sparse representation, which is less than half of the required bits for the naive sparse representation, when DNN architectures are considered.

4.3.2 Quantized Representation

For the quantized representation we consider a framework building upon the scaled sign operator (Karimireddy et al., 2019; Zheng et al., 2019), which returns the quantized representation of a vector \mathbf{v} as

$$\mathcal{Q}(\mathbf{v}) = \|\mathbf{v}\|_1/d \cdot \text{sign}(\mathbf{v}), \quad (17)$$

where d is the dimension of vector \mathbf{v} . Further, it has been shown that when the vector is divided into smaller blocks and quantization is applied to each block separately, it is possible to reduce the quantization error further (Zheng et al., 2019). Inspired by the natural compression approach in (Horvath et al., 2019), and the aforementioned blockwise quantization strategy in (Zheng et al., 2019), we employ a fractional quantization strategy. The fractional quantization scheme works as follows: first, it identifies the maximum and minimum values in $|\mathbf{v}|$, denoted by v_{max} and v_{min} , respectively, then for the given bit budget q the interval $[v_{max}, v_{min}]$ is divided into $L = 2^{q-1}$ subintervals I_1, \dots, I_L such that

$$I_l = \left[\frac{v_{max}}{\alpha^{l-1}}, \frac{v_{max}}{\alpha^l} \right], \quad (18)$$

where $\alpha = (v_{max}/v_{min})^{1/L}$.

Hence, for the quantized representation of each value in $|\mathbf{v}|$, we use index of the corresponding interval using $q - 1$ bits and one more bit for the sign, thus q bits in total. After forming a bitstream of the quantized representation we append L mean values μ_1, \dots, μ_L , to the end, where μ_l is the average of the values in $|\mathbf{v}|$, which falls into the subinterval I_l . Hence, the recovered values at the receiver side takes values from the set $\{\mu_1, \dots, \mu_L\}$.

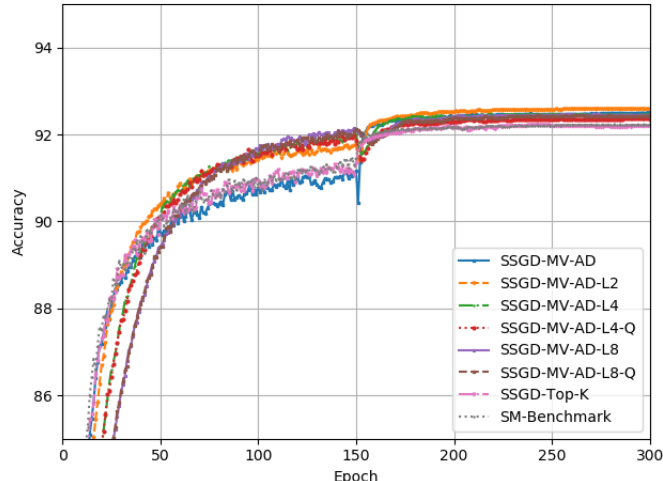


Figure 2. Test accuracy results over 300 epochs for SSGD-MV-AD variations, SSGD-top- K and SM benchmarks.

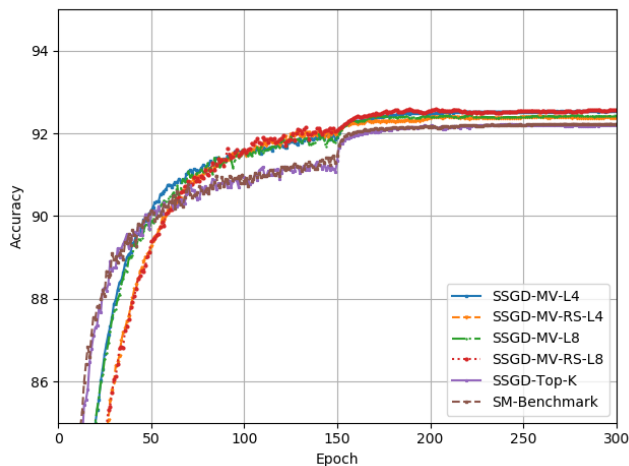


Figure 3. Test accuracy results over 300 epochs for SSGD-MV, SSGD-MV-RS, SSGD-top- K and the SM benchmark.

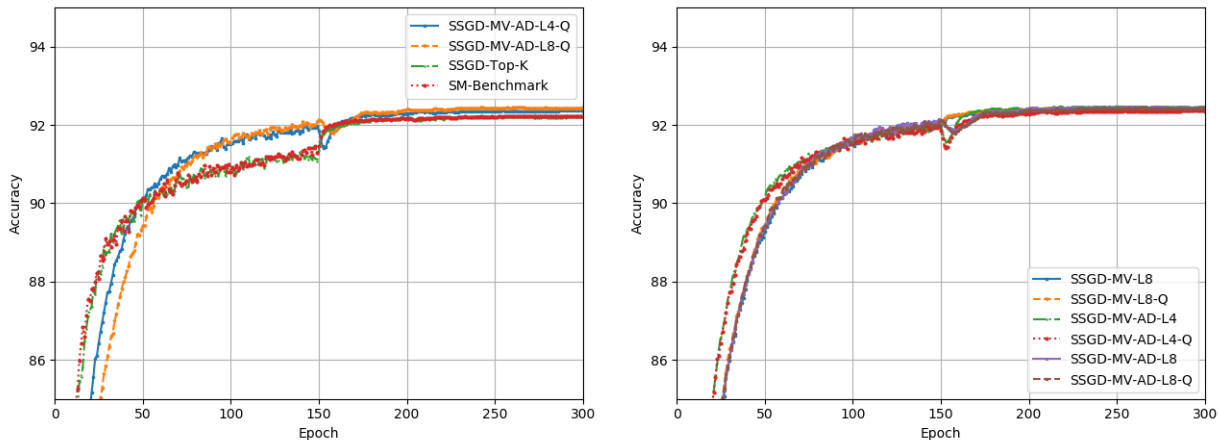
4.4 Simulation Results

As explained in Section 4.2, in total we consider three different variations of the introduced majority voting strategy with 13 different implementations in total. We provide all the corresponding top-1 test accuracy results and the achieved compression rates both in the uplink and downlink direction in Table 1. To provide a better understanding of the compression rates given in Table 1, we also provide the effective bit budgets used for representing the quantized values and the non-zero positions of the sparse vector, which are denoted by \bar{q}_{val} and \bar{q}_{loc} respectively. We note that \bar{q}_{val} and \bar{q}_{loc} are equivalent to Q_{val}/dH and Q_{loc}/dH , respectively.

In Figures 1 and 2, we illustrated the effects of the local steps for SSGD-MV and SSG-MV-AD, respectively. From these

figures we can see that the benefits of local SGD steps are not limited to the communication load; but it also helps with the convergence as the local step number reaching higher H values. This is apparent for SSGD-MV in Figure 1. but it is most prominent for the SSGD-MV-AD by preventing the accuracy drops at epoch 150 which where we decay the starting learning rate for the first time as shown at Figure 2. Aside from the healthier convergence, Table 1 shows that local steps of $H = 2, 4$ also benefits to the consistency of the results by achieving lower standard deviation in their own algorithm types and also compression rate is multiply by 2 with each consecutive even local steps. In Figure 3, we observe that SSGD-MV-RS performs similarly to the SSGD-MV, although still outperforms the benchmark algorithms.

In Figures 4, we monitor the impact of quantization on the



(a) Comparison of the SSGD-MV variations, in high compression regime, and the benchmark schemes. (b) Comparison of the test accuracy results of SSGD-MV strategies with and without quantization.

Figure 4. Test accuracy results over 300 epochs when quantization is employed.

test accuracy of the SSGD-MV strategy. In Figure 4b, we plot the test accuracy results of the 3 SSGD-MV variations namely SSGD-MV-L8, SSGD-MV-AD-L4, SSGD-MV-AD-L8, and their quantized versions. We observe from the figure that the quantization has a very minor impact on the test accuracy, although it reduces the number of bits used for representing the each non-zero value by factor of 8. In Figure 4a, we compare the two majority voting based schemes that achieve the highest compression rates namely, SSGD-MV-AD-L4-Q and SSGD-MV-AD-L8-Q, with the two benchmark schemes to demonstrate that even with high compression rates majority voting strategy outperforms the benchmark schemes.

From the simulation results, we observe that SSGD-MV-AD-L2 achieves the highest test accuracy, which may seem counter-intuitive at first glance, from the communication load- accuracy trade-off perspective, since both add-drop mechanism and local steps are used to reduce the communication load. However, it has been shown that local SGD may achieve higher performance compared to the mini-batch alternative (Lin et al., 2020b; Woodworth et al., 2020). Besides, the use of local steps increases the accuracy of the voting mechanism since the variations in the values over H local steps provides more reliable information for identifying the most important positions compared to the single gradient estimate, due to the randomness in the stochastic gradient computations. This interpretation is also supported by the comparison of the test accuracy results of SSGD-MV, SSGD-MV-L2, SSGD-MV-L4, and SSGD-MV-L8, where the highest test accuracy is achieved by SSGD-MV-L4. These observations are also consistent with the previous findings on the performance of local SGD, where the test accuracy first increases with the number of

local steps H , but then starts to decline after a certain point. We also note that one disadvantage of using larger H is causing delay in the error accumulation, so that the error aggregated for the local difference becomes outdated.

According to the simulation results, SSGD-MV-AD-L2 outperforms SSGD-MV-L2. We argue that, as briefly discussed in Section 3, the introduced add-drop mechanism, in addition to reducing the communication load, also acts as a natural regularizer for NN training, and thus serves to achieve better generalization. As we already mentioned above, the use of local steps improves the performance of the voting mechanism, which explains the difference between the accuracy of SSGD-MV-AD-L2 and SSGD-MV-AD.

In our simulations, we also combine the proposed majority voting based sparsification approach with the quantization strategy to reduce the communication load further and observe that it is possible to achieve up to $\times 4000$ compression in total, using SSGD-MV-AD-L8-Q4, without a noticeable loss in the test accuracy compared to the SM benchmark. Finally, we want to remark that the achieved accuracy results can be improved further by employing accelerated SGD variants, such as momentum SGD or/and applying layer-wise sparsification instead of using a global one (Eghlidi & Jaggi, 2020). We will consider these extensions as future work.

5 CONCLUSION

In this paper, we introduced a majority voting based sparse communication strategy for the DSGD framework. The proposed majority voting strategy, particularly the one enriched

Table 1. Top-1 test accuracy and the compression rate of the studied schemes. Schemes with the highest test accuracy and the highest compression rate are highlighted in **bold**.

Method	Top-1 Accuracy (mean \pm std)	Uplink bit budget	Downlink bit budget	Compression Rate Uplink/ Downlink
SSGD-MV	92.36 \pm 0.21	$\bar{q}_{loc} = 9 \times 10^{-2}$ $\bar{q}_{val} = 3.2 \times 10^{-1}$	$\bar{q}_{loc} = 9 \times 10^{-2}$, $\bar{q}_{val} = 3.2 \times 10^{-1}$	$\times 78 / \times 78$
SSGD-MV-L2	92.5 \pm 0.15	$\bar{q}_{loc} = 4.5 \times 10^{-2}$, $\bar{q}_{val} = 1.6 \times 10^{-1}$	$\bar{q}_{loc} = 4.5 \times 10^{-2}$, $\bar{q}_{val} = 1.6 \times 10^{-1}$	$\times 156 / \times 156$
SSGD-MV-L4	92.54 \pm 0.27	$\bar{q}_{loc} = 2.25 \times 10^{-2}$, $\bar{q}_{val} = 8 \times 10^{-2}$	$\bar{q}_{loc} = 2.25 \times 10^{-2}$, $\bar{q}_{val} = 8 \times 10^{-2}$	$\times 312 / \times 312$
SSGD-MV-L8	92.37 \pm 0.17	$\bar{q}_{loc} = 1.125 \times 10^{-2}$, $\bar{q}_{val} = 4 \times 10^{-2}$	$\bar{q}_{loc} = 1.125 \times 10^{-2}$, $\bar{q}_{val} = 4 \times 10^{-2}$	$\times 624 / \times 624$
SSGD-MV-L8-Q	92.43 \pm 0.14	$\bar{q}_{loc} = 1.125 \times 10^{-2}$, $\bar{q}_{val} = 5 \times 10^{-3}$	$\bar{q}_{loc} = 1.125 \times 10^{-2}$, $\bar{q}_{val} = 4 \times 10^{-2}$	$\times 2000 / \times 624$
SSGD-MV-RS-L4	92.43 \pm 0.2	$\bar{q}_{loc} = 2.25 \times 10^{-2}$, $\bar{q}_{val} = 8 \times 10^{-2}$	$\bar{q}_{loc} = 2.25 \times 10^{-2}$, $\bar{q}_{val} = 8 \times 10^{-2}$	$\times 312 / \times 312$
SSGD-MV-RS-L8	92.57 \pm 0.24	$\bar{q}_{loc} = 2.25 \times 10^{-2}$, $\bar{q}_{val} = 8 \times 10^{-2}$	$\bar{q}_{loc} = 2.25 \times 10^{-2}$, $\bar{q}_{val} = 8 \times 10^{-2}$	$\times 624 / \times 624$
SSGD-MV-AD	92.5 \pm 0.19	$\bar{q}_{loc} = 2.4 \times 10^{-2}$ $\bar{q}_{val} = 3.2 \times 10^{-1}$	$\bar{q}_{loc} = 9 \times 10^{-2}$, $\bar{q}_{val} = 3.2 \times 10^{-1}$	$\times 93 / \times 78$
SSGD-MV-AD-L2	92.6 \pm 0.19	$\bar{q}_{loc} = 1.2 \times 10^{-2}$ $\bar{q}_{val} = 1.6 \times 10^{-1}$	$\bar{q}_{loc} = 4.5 \times 10^{-2}$, $\bar{q}_{val} = 1.6 \times 10^{-1}$	$\times 186 / \times 156$
SSGD-MV-AD-L4	92.46 \pm 0.22	$\bar{q}_{loc} = 6 \times 10^{-3}$ $\bar{q}_{val} = 8 \times 10^{-2}$	$\bar{q}_{loc} = 2.25 \times 10^{-2}$, $\bar{q}_{val} = 8 \times 10^{-2}$	$\times 372 / \times 312$
SSGD-MV-AD-L4-Q	92.36 \pm 0.19	$\bar{q}_{loc} = 6 \times 10^{-3}$ $\bar{q}_{val} = 1 \times 10^{-2}$	$\bar{q}_{loc} = 2.25 \times 10^{-2}$, $\bar{q}_{val} = 8 \times 10^{-2}$	$\times 2000 / \times 312$
SSGD-MV-AD-L8	92.45 \pm 0.2	$\bar{q}_{loc} = 3 \times 10^{-3}$ $\bar{q}_{val} = 4 \times 10^{-2}$	$\bar{q}_{loc} = 1.125 \times 10^{-2}$, $\bar{q}_{val} = 4 \times 10^{-2}$	$\times 745 / \times 624$
SSGD-MV-AD-L8-Q	92.43 \pm 0.23	$\bar{q}_{loc} = 3 \times 10^{-3}$ $\bar{q}_{val} = 5 \times 10^{-3}$	$\bar{q}_{loc} = 1.125 \times 10^{-2}$, $\bar{q}_{val} = 4 \times 10^{-2}$	$\times 4000 / \times 624$
SSGD-top- K	92.194 \pm 0.324	$\bar{q}_{loc} = 9 \times 10^{-2}$ $\bar{q}_{val} = 3.2 \times 10^{-1}$	$\bar{q}_{loc} = 6 \times 10^{-1}$ $\bar{q}_{val} = 3.2$	$\times 78 / \times 8.4$
SM-Benchmark	92.228 \pm 0.232	-	-	-

with the add-drop mechanism, has three main benefits: First, it reduces the communication load further by taking advantage of the correlation among the model updates across iterations. Second, it serves as a natural regularization on the NN sparsity to achieve better generalization, and finally it works as a linear operator. By conducting extensive simulations, we showed that the proposed SSGD-MV strategy (and its variants) achieves the benchmark test accuracy of a single machine. When combined with localization and quantization strategies, it can achieve impressive compression rates as high as $\times 4000$.

REFERENCES

Abad, M. S. H., Ozfatura, E., Gunduz, D., and Ercetin, O. Hierarchical federated learning across heterogeneous

cellular networks. In *ICASSP 2020 - 2020 IEEE International Conference on Acoustics, Speech and Signal Processing (ICASSP)*, pp. 8866–8870, 2020.

Aji, A. F. and Heafield, K. Sparse communication for distributed gradient descent. In *Proceedings of the 2017 Conference on Empirical Methods in Natural Language Processing*, pp. 440–445, Copenhagen, Denmark, September 2017. Association for Computational Linguistics. doi: 10.18653/v1/D17-1045. URL <https://www.aclweb.org/anthology/D17-1045>.

Alistarh, D., Grubic, D., Li, J., Tomioka, R., and Vojnovic, M. Qsgd: Communication-efficient sgd via gradient quantization and encoding. In Guyon, I., Luxburg, U. V., Bengio, S., Wallach, H., Fergus, R., Vishwanathan, S., and Garnett, R. (eds.), *Advances in Neural Information Pro-*

- cessing Systems 30*, pp. 1709–1720. Curran Associates, Inc., 2017.
- Alistarh, D., Hoefler, T., Johansson, M., Konstantinov, N., Khirirat, S., and Renggli, C. The convergence of sparsified gradient methods. In Bengio, S., Wallach, H., Larochelle, H., Grauman, K., Cesa-Bianchi, N., and Garnett, R. (eds.), *Advances in Neural Information Processing Systems 31*, pp. 5976–5986. Curran Associates, Inc., 2018.
- Barnes, L. P., Inan, H. A., Isik, B., and Ozgur, A. rtop-k: A statistical estimation approach to distributed sgd, 2020.
- Bernstein, J., Wang, Y.-X., Azizzadenesheli, K., and Anandkumar, A. signSGD: Compressed optimisation for non-convex problems. In Dy, J. and Krause, A. (eds.), *Proceedings of the 35th International Conference on Machine Learning*, volume 80 of *Proceedings of Machine Learning Research*, pp. 560–569, Stockholm Småstugan, Stockholm Sweden, 10–15 Jul 2018. PMLR. URL <http://proceedings.mlr.press/v80/bernstein18a.html>.
- Bernstein, J., Zhao, J., Azizzadenesheli, K., and Anandkumar, A. signSGD with majority vote is communication efficient and fault tolerant. In *International Conference on Learning Representations*, 2019. URL <https://openreview.net/forum?id=BJxhijAcY7>.
- Dean, J., Corrado, G. S., Monga, R., Chen, K., Devin, M., Le, Q. V., Mao, M. Z., Ranzato, M., Senior, A., Tucker, P., Yang, K., and Ng, A. Y. Large scale distributed deep networks. In *Proceedings of the 25th International Conference on Neural Information Processing Systems - Volume 1*, NIPS’12, pp. 1223–1231, USA, 2012. Curran Associates Inc.
- Dekel, O., Gilad-Bachrach, R., Shamir, O., and Xiao, L. Optimal distributed online prediction using mini-batches. *J. Mach. Learn. Res.*, 13(1):165–202, January 2012.
- Dieuleveut, A. and Patel, K. K. Communication trade-offs for local-sgd with large step size. In Wallach, H., Larochelle, H., Beygelzimer, A., d’Alché-Buc, F., Fox, E., and Garnett, R. (eds.), *Advances in Neural Information Processing Systems 32*, pp. 13601–13612. Curran Associates, Inc., 2019. URL <http://papers.nips.cc/paper/9512-communication-trade-offs-for-local-sgd-with-large-step-size.pdf>.
- Eghlidi, N. F. and Jaggi, M. Sparse communication for training deep networks, 2020.
- Elibol, M., Lei, L., and Jordan, M. I. Variance reduction with sparse gradients. In *International Conference on Learning Representations*, 2020. URL <https://openreview.net/forum?id=Syx1DkSYwB>.
- Frankle, J. and Carbin, M. The lottery ticket hypothesis: Finding sparse, trainable neural networks. In *International Conference on Learning Representations*, 2019. URL <https://openreview.net/forum?id=rJl-b3RcF7>.
- Goyal, P., Dollár, P., Girshick, R. B., Noordhuis, P., Wesolowski, L., Kyrola, A., Tulloch, A., Jia, Y., and He, K. Accurate, large minibatch SGD: training imagenet in 1 hour. *CoRR*, abs/1706.02677, 2017. URL <http://arxiv.org/abs/1706.02677>.
- Haddadpour, F., Kamani, M. M., Mahdavi, M., and Cadambe, V. Local sgd with periodic averaging: Tighter analysis and adaptive synchronization. In Wallach, H., Larochelle, H., Beygelzimer, A., d’Alché-Buc, F., Fox, E., and Garnett, R. (eds.), *Advances in Neural Information Processing Systems 32*, pp. 11082–11094. Curran Associates, Inc., 2019. URL <http://papers.nips.cc/paper/9288-local-sgd-with-periodic-averaging-tighter-analysis-and-adaptive-synchronization.pdf>.
- He, K., Zhang, X., Ren, S., and Sun, J. Deep residual learning for image recognition. In *2016 IEEE Conference on Computer Vision and Pattern Recognition (CVPR)*, pp. 770–778, 2016.
- He, K., Zhang, X., Ren, S., and Sun, J. Identity mappings in deep residual networks. In Leibe, B., Matas, J., Sebe, N., and Welling, M. (eds.), *Computer Vision – ECCV 2016*, pp. 630–645, Cham, 2016. Springer International Publishing.
- Horvath, S., Ho, C., Horvath, L., Sahu, A. N., Canini, M., and Richtárik, P. Natural compression for distributed deep learning. *CoRR*, abs/1905.10988, 2019. URL <http://arxiv.org/abs/1905.10988>.
- Huang, G., Liu, Z., van der Maaten, L., and Weinberger, K. Q. Densely connected convolutional networks. In *Proceedings of the IEEE Conference on Computer Vision and Pattern Recognition (CVPR)*, July 2017.
- Jiang, P. and Agrawal, G. A linear speedup analysis of distributed deep learning with sparse and quantized communication. In Bengio, S., Wallach, H., Larochelle, H., Grauman, K., Cesa-Bianchi, N., and Garnett, R. (eds.), *Advances in Neural Information Processing Systems 31*, pp. 2529–2540. Curran Associates, Inc., 2018.

- Karimireddy, S. P., Rebjock, Q., Stich, S., and Jaggi, M. Error feedback fixes SignSGD and other gradient compression schemes. In Chaudhuri, K. and Salakhutdinov, R. (eds.), *Proceedings of the 36th International Conference on Machine Learning*, volume 97 of *Proceedings of Machine Learning Research*, pp. 3252–3261, Long Beach, California, USA, 09–15 Jun 2019. PMLR. URL <http://proceedings.mlr.press/v97/karimireddy19a.html>.
- Khaled, A., Mishchenko, K., and Richtárik, P. Tighter theory for local sgd on identical and heterogeneous data, 2020.
- Krizhevsky, A., Nair, V., and Hinton, G. Cifar-10 (canadian institute for advanced research). URL <http://www.cs.toronto.edu/~kriz/cifar.html>.
- Li, M., Andersen, D. G., Park, J. W., Smola, A. J., Ahmed, A., Josifovski, V., Long, J., Shekita, E. J., and Su, B.-Y. Scaling distributed machine learning with the parameter server. In *Proceedings of the 11th USENIX Conference on Operating Systems Design and Implementation, OSDI'14*, pp. 583–598, Berkeley, CA, USA, 2014. USENIX Association. ISBN 978-1-931971-16-4.
- Lin, T., Stich, S. U., Barba, L., Dmitriev, D., and Jaggi, M. Dynamic model pruning with feedback. In *International Conference on Learning Representations, 2020a*. URL <https://openreview.net/forum?id=SJem81SFwB>.
- Lin, T., Stich, S. U., Patel, K. K., and Jaggi, M. Don't use large mini-batches, use local sgd. In *International Conference on Learning Representations, 2020b*. URL <https://openreview.net/forum?id=Bley01BFPr>.
- Lin, Y., Han, S., Mao, H., Wang, Y., and Dally, B. Deep gradient compression: Reducing the communication bandwidth for distributed training. In *International Conference on Learning Representations, 2018*.
- McMahan, B., Moore, E., Ramage, D., Hampson, S., and y Arcas, B. A. Communication-Efficient Learning of Deep Networks from Decentralized Data. In Singh, A. and Zhu, J. (eds.), *Proceedings of the 20th International Conference on Artificial Intelligence and Statistics*, volume 54 of *Proceedings of Machine Learning Research*, pp. 1273–1282, Fort Lauderdale, FL, USA, 20–22 Apr 2017. PMLR. URL <http://proceedings.mlr.press/v54/mcmahan17a.html>.
- Mohammadi Amiri, M. and Gündüz, D. Machine learning at the wireless edge: Distributed stochastic gradient descent over-the-air. *IEEE Transactions on Signal Processing*, 68:2155–2169, 2020.
- Mostafa, H. and Wang, X. Parameter efficient training of deep convolutional neural networks by dynamic sparse reparameterization. In Chaudhuri, K. and Salakhutdinov, R. (eds.), *Proceedings of the 36th International Conference on Machine Learning*, volume 97 of *Proceedings of Machine Learning Research*, pp. 4646–4655, Long Beach, California, USA, 09–15 Jun 2019. PMLR. URL <http://proceedings.mlr.press/v97/mostafa19a.html>.
- Sattler, F., Wiedemann, S., Müller, K., and Samek, W. Robust and communication-efficient federated learning from non-i.i.d. data. *IEEE Transactions on Neural Networks and Learning Systems*, pp. 1–14, 2019.
- Seide, F., Fu, H., Droppo, J., Li, G., and Yu, D. 1-bit stochastic gradient descent and application to data-parallel distributed training of speech dnns. In *Interspeech 2014*, September 2014. URL <https://www.microsoft.com/en-us/research/publication/1-bit-stochastic-gradient-descent-and-application-to-data-parallel-distributed-training-of-speech-dnns/>.
- Sery, T. and Cohen, K. On analog gradient descent learning over multiple access fading channels. *IEEE Trans. Signal Proc.*, 68:2897–2911, 2020.
- Shi, S., Wang, Q., Zhao, K., Tang, Z., Wang, Y., Huang, X., and Chu, X. A distributed synchronous sgd algorithm with global top-k sparsification for low bandwidth networks. In *2019 IEEE 39th International Conference on Distributed Computing Systems (ICDCS)*, pp. 2238–2247, 2019.
- Simonyan, K. and Zisserman, A. Very deep convolutional networks for large-scale image recognition. In *International Conference on Learning Representations, 2015*.
- Stich, S. U. Local SGD converges fast and communicates little. In *International Conference on Learning Representations, 2019*. URL <https://openreview.net/forum?id=Slg2JnRcFX>.
- Stich, S. U., Cordonnier, J.-B., and Jaggi, M. Sparsified sgd with memory. In Bengio, S., Wallach, H., Larochelle, H., Grauman, K., Cesa-Bianchi, N., and Garnett, R. (eds.), *Advances in Neural Information Processing Systems 31*, pp. 4448–4459. Curran Associates, Inc., 2018.
- Tang, H., Yu, C., Lian, X., Zhang, T., and Liu, J. DoubleSqueeze: Parallel stochastic gradient descent with double-pass error-compensated compression. In Chaudhuri, K. and Salakhutdinov, R. (eds.), *Proceedings of the 36th International Conference on Machine Learning*

- Learning*, volume 97 of *Proceedings of Machine Learning Research*, pp. 6155–6165, Long Beach, California, USA, 09–15 Jun 2019. PMLR. URL <http://proceedings.mlr.press/v97/tang19d.html>.
- Wang, J. and Joshi, G. Cooperative SGD: A unified framework for the design and analysis of communication-efficient SGD algorithms. *CoRR*, abs/1808.07576, 2018. URL <http://arxiv.org/abs/1808.07576>.
- Wang, S., Tuor, T., Salonidis, T., Leung, K. K., Makaya, C., He, T., and Chan, K. Adaptive federated learning in resource constrained edge computing systems. *IEEE Journal on Selected Areas in Communications*, 37(6): 1205–1221, 2019.
- Wangni, J., Wang, J., Liu, J., and Zhang, T. Gradient sparsification for communication-efficient distributed optimization. In Bengio, S., Wallach, H., Larochelle, H., Grauman, K., Cesa-Bianchi, N., and Garnett, R. (eds.), *Advances in Neural Information Processing Systems 31*, pp. 1305–1315. Curran Associates, Inc., 2018.
- Wen, W., Xu, C., Yan, F., Wu, C., Wang, Y., Chen, Y., and Li, H. Terngrad: Ternary gradients to reduce communication in distributed deep learning. In Guyon, I., Luxburg, U. V., Bengio, S., Wallach, H., Fergus, R., Vishwanathan, S., and Garnett, R. (eds.), *Advances in Neural Information Processing Systems 30*, pp. 1509–1519. Curran Associates, Inc., 2017.
- Woodworth, B., Patel, K. K., Stich, S. U., Dai, Z., Bullins, B., McMahan, H. B., Shamir, O., and Srebro, N. Is local sgd better than minibatch sgd?, 2020.
- Wu, J., Huang, W., Huang, J., and Zhang, T. Error compensated quantized SGD and its applications to large-scale distributed optimization. In Dy, J. and Krause, A. (eds.), *Proceedings of the 35th International Conference on Machine Learning*, volume 80 of *Proceedings of Machine Learning Research*, pp. 5325–5333, Stockholmsmässan, Stockholm Sweden, 10–15 Jul 2018a. PMLR. URL <http://proceedings.mlr.press/v80/wu18d.html>.
- Wu, J., Huang, W., Huang, J., and Zhang, T. Error compensated quantized SGD and its applications to large-scale distributed optimization. In Dy, J. and Krause, A. (eds.), *Proceedings of the 35th International Conference on Machine Learning*, volume 80 of *Proceedings of Machine Learning Research*, pp. 5325–5333, Stockholmsmässan, Stockholm Sweden, 10–15 Jul 2018b. PMLR.
- Yu, H., Yang, S., and Zhu, S. Parallel restarted sgd with faster convergence and less communication: Demystifying why model averaging works for deep learning, 2018.
- Yu, H., Jin, R., and Yang, S. On the linear speedup analysis of communication efficient momentum SGD for distributed non-convex optimization. In Chaudhuri, K. and Salakhutdinov, R. (eds.), *Proceedings of the 36th International Conference on Machine Learning*, volume 97 of *Proceedings of Machine Learning Research*, pp. 7184–7193, Long Beach, California, USA, 09–15 Jun 2019a.
- Yu, Y., Wu, J., and Huang, L. Double quantization for communication-efficient distributed optimization. In *Advances in Neural Information Processing Systems 32*, pp. 4438–4449. Curran Associates, Inc., 2019b. URL <http://papers.nips.cc/paper/8694-double-quantization-for-communication-efficient-distributed-optimization.pdf>.
- Zheng, S., Huang, Z., and Kwok, J. Communication-efficient distributed blockwise momentum sgd with error-feedback. In *Advances in Neural Information Processing Systems 32*, pp. 11450–11460. Curran Associates, Inc., 2019.
- Zhou, F. and Cong, G. On the convergence properties of a k-step averaging stochastic gradient descent algorithm for nonconvex optimization. In *Proceedings of the Twenty-Seventh International Joint Conference on Artificial Intelligence, IJCAI-18*, pp. 3219–3227. International Joint Conferences on Artificial Intelligence Organization, 7 2018.
- Zhu, G., Wang, Y., and Huang, K. Broadband analog aggregation for low-latency federated edge learning. *IEEE Trans. Wireless Comms.*, 2019.
- Zinkevich, M. A., Weimer, M., Smola, A., and Li, L. Parallelized stochastic gradient descent. In *Proceedings of the 23rd International Conference on Neural Information Processing Systems - Volume 2, NIPS’10*, pp. 2595–2603, USA, 2010.